

Semi-active tuned liquid column dampers for vibration control of structures

Swaroop K. Yalla ^{a,*}, Ahsan Kareem ^b, Jeffrey C. Kantor ^c

^a NatHaz Modeling Laboratory, Department of Civil Engineering and Geological Sciences, University of Notre Dame, Notre Dame, IN 46556, USA

^b Department of Civil Engineering and Geological Sciences, University of Notre Dame, Notre Dame, IN 46556, USA

^c Department of Chemical Engineering, University of Notre Dame, Notre Dame, IN 46556, USA

Received 18 February 2000; received in revised form 12 March 2001; accepted 19 April 2001

Abstract

Semi-active systems are attractive for structural control applications because they offer some of the best features of both passive and active systems. This paper examines a passive tuned liquid column damper which is converted into a variable-damping semi-active system. Different semi-active algorithms based on the clipped-optimal and fuzzy control strategies are studied using numerical examples. The main objective of this paper is to study the effectiveness of different control algorithms for semi-active tuned liquid dampers for structural control applications. © 2001 Elsevier Science Ltd. All rights reserved.

Keywords: Tuned liquid column dampers; Structural control, semi-active; Wind; Clipped-optimal; On-off control; Fuzzy control; Variable-damping devices

1. Introduction

The focus of recent research in structural control has shifted from active systems to semi-active devices for mitigating structural response. Semi-active control devices do not introduce mechanical energy into the controlled structural system; rather they manipulate system properties in an optimal manner to reduce the structural response [1]. A semi-active system originates primarily from a passive control system with an option to modify its physical properties according to a prescribed control law.

Semi-active control systems were first studied for civil engineering structures by Hrovat et al. [2] In other fields, such as automotive vibration control, considerable research has been done on semi-active systems [3,4]. A number of devices are currently being studied in the area of structural control, namely variable-stiffness devices, controllable fluid dampers, friction control devices, fluid

viscous devices, etc. Recent papers in this area provide a state-of-the-art review on semi-active control devices for vibration control of structures [5–7].

Tuned liquid column dampers (TLCDs) are a special type of tuned liquid damper (TLD) that rely on the motion of the liquid column in a U-shaped tube to counteract the action of external forces acting on the structure. The inherent damping is introduced in the oscillating liquid column through an orifice. Sakai and Takaeda [8] proposed the passive TLCD and carried out experiments to validate the analytical model. Subsequent numerical studies found TLCDs to be effective for wind and earthquake loading [9,10]. Such studies mainly dealt with passive versions of TLCDs with no option to control the damper characteristics. Recently, semi-active and active TLCD systems have been proposed and studied by Kareem [11], Haroun and Pires [12], Abe et al. [32] and Yalla et al. [13]. In particular, Yalla and Kareem [14] discuss a *controllable passive* system in which the headloss coefficient is changed adaptively in response to change in excitation in order to maintain the optimal damping in the TLCD.

In this paper, a variable-damping tuned liquid column damper is studied in a semi-active framework. Different

* Corresponding author. Tel.: +1-219-631-4308; fax: +1-219-631-9236.

E-mail addresses: syalla@nd.edu (S.K. Yalla), kareem@nd.edu (A. Kareem), jeff.1@nd.edu (J.C. Kantor).

semi-active algorithms such as the clipped-optimal *continuously varying* and *on-off* strategies are studied and compared. Numerical examples are presented: the first example examines a multiple-degree-of-freedom (MDOF) system combined with a TLCD subjected to harmonic excitation controlled using three types of control strategy: (1) full state feedback; (2) observer-based feedback; and (3) fuzzy control. The second example discusses an MDOF-TLCD system subjected to random wind excitation controlled using full state feedback. Finally, the effect of inclusion of TLCD orifice valve dynamics on the response of the structure is examined.

2. Semi-active TLCD system

The equations of motion of the combined TLCD–structure can be written as

$$\begin{bmatrix} \mathbf{M}_s+m_f & \alpha m_f \\ \alpha m_f & m_f \end{bmatrix} \begin{bmatrix} \ddot{\mathbf{X}}_s \\ \ddot{X}_f \end{bmatrix} + \begin{bmatrix} \mathbf{C}_s & 0 \\ 0 & \frac{\rho A \xi |\dot{X}_f|}{2} \end{bmatrix} \begin{bmatrix} \dot{\mathbf{X}}_s \\ \dot{X}_f \end{bmatrix} + \begin{bmatrix} \mathbf{K}_s & 0 \\ 0 & k_f \end{bmatrix} \begin{bmatrix} \mathbf{X}_s \\ X_f \end{bmatrix} = \begin{bmatrix} \mathbf{F}(t) \\ 0 \end{bmatrix}; \quad |X_f| \leq \frac{(l-b)}{2}, \quad (1)$$

where

\mathbf{X}_s	displacement of the primary system
X_f	displacement of the liquid in the damper
\mathbf{M}_s	mass of the primary system
\mathbf{K}_s	stiffness of the primary system
\mathbf{C}_s	damping coefficient of the primary system
k_f	“stiffness” of the liquid column ($=2\rho Ag$)
m_f	mass of liquid in the tube ($=\rho Al$)
ρ	liquid density
A	cross-sectional area of the tube
ω_f	natural frequency of the liquid damper ($=\sqrt{k_f/m_f}=\sqrt{2g/l}$)
α	length ratio ($=b/l$)
l	length of the liquid column
b	horizontal length of the column
g	gravitational constant
$\mathbf{F}(t)$	external force acting on the primary mass.

The constraint in Eq. (1) is imposed because the U-shaped configuration of the liquid column must be maintained in order for the damper to perform effectively (i.e., fluid must remain in the vertical portions of the U-shaped tube at all times).

The semi-active system described in this paper requires a controllable orifice with negligible valve dynamics whose coefficient of headloss (or the orifice

opening) can be changed continuously by applying a command voltage (Fig. 1). The damping force is translated into an active force which controls structural motions. Eq. (1) can be recast in an active control framework as follows

$$\begin{bmatrix} \mathbf{M}_s+m_f & \alpha m_f \\ \alpha m_f & m_f \end{bmatrix} \begin{bmatrix} \ddot{\mathbf{X}}_s \\ \ddot{X}_f \end{bmatrix} + \begin{bmatrix} \mathbf{C}_s & 0 \\ 0 & 0 \end{bmatrix} \begin{bmatrix} \dot{\mathbf{X}}_s \\ \dot{X}_f \end{bmatrix} + \begin{bmatrix} \mathbf{K}_s & 0 \\ 0 & k_f \end{bmatrix} \begin{bmatrix} \mathbf{X}_s \\ X_f \end{bmatrix} = \begin{bmatrix} \mathbf{F}(t) \\ 0 \end{bmatrix} + \begin{bmatrix} 0 \\ 1 \end{bmatrix} u(t), \quad (2)$$

where the control force $u(t)$ is given by

$$u(t) = -\frac{\rho A \xi(t) |\dot{X}_f|}{2} \dot{X}_f. \quad (3)$$

The coefficient of headloss is an important parameter that is controlled by varying the orifice area of the valve. In the case of a passive system, this headloss coefficient is unchanged. The headloss through a valve/orifice is defined as

$$h_l = \frac{\xi V^2}{2g}, \quad (4)$$

where V is the liquid velocity and ξ is the coefficient of headloss. The coefficients of headloss for different valve openings are well documented for different types of valves [15]. Most valve suppliers provide the characteristic curves for orifice opening and the valve conductance (C_v). The relationship between the headloss coefficient (ξ) and the valve conductance (C_v) is derived in Appendix A for circular cross-sections.

The damping force in a semi-active TLCD can be written as

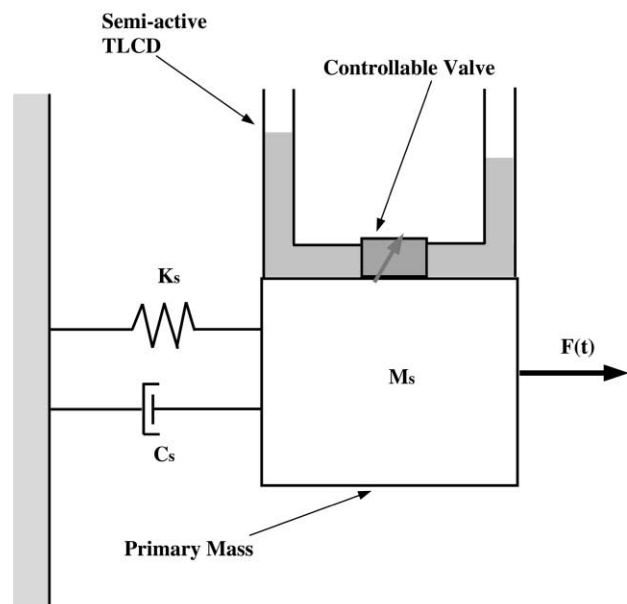


Fig. 1. Semi-active TLCD–structure combined system.

$$F_d(t) = \frac{\rho A \xi(\Lambda, t)}{2} |\dot{X}_r(t)| \dot{X}_r(t), \quad (5)$$

where $\xi(\Lambda, t)$ is the headloss coefficient, which is a function of the applied voltage Λ at a given time t . Eq. (5) can be written as

$$F_d(t) = \tilde{C}(\Lambda, t) |V| V, \quad (6)$$

where $\tilde{C}(\Lambda, t) = [\rho A \xi(\Lambda, t)]/2$ and $V = \dot{X}_r(t)$. This damper system can be compared with a typical variable-damping fluid damper. Semi-active versions of fluid viscous dampers have been studied by Symans and Constantinou [16] and Patten et al. [17], amongst others. The damping force in such a system can be written as

$$F(t) = C(\Lambda, t) \tilde{V}, \quad (7)$$

where $C(\Lambda)$ is the damping coefficient, which is a function of the command voltage Λ , and \tilde{V} is the velocity of the piston head. The damping coefficient is bounded by a maximum and a minimum value and may take any value between these bounds.

Comparing Eqs. (6) and (7), one can note the basic similarities in the fundamental operation of these dampers. However, there are some primary differences between the two physical systems. In variable-orifice dampers the fluid is viscous, usually some silicone-based material, which is pushed through an orifice by a piston. In the TLCDC case, the liquid is usually water under atmospheric pressure. Moreover, the damping introduced by an orifice in a TLCDC system is quadratic, whereas the damping imparted by a fluid damper is linear [18].

3. Control strategies

Most semi-active devices (for e.g., MR and ER dampers, semi-active TLCDCs, etc.) are intrinsically non-linear, which makes it challenging to develop control strategies to optimally exploit their unique features. Some of the common examples of such algorithms are sliding mode control and non-linear H_∞ strategies [19]. Another innovative algorithm involving shaping of the force–deformation loop in the variable damper is reported by Kurino and Kobori [20]. Other researchers have used fuzzy control schemes to effectively implement semi-active control (e.g., [21,22]).

The first strategy considered in this paper is based on LQR/LQG type control based on optimal control theory. The negative sign in Eq. (3) ensures that the control force is always acting in a direction opposite to the liquid velocity. In the case that the liquid velocity and the desired control force are of the same sign, Eq. (3) implies that ξ is negative. Since it is not practical to have a negative coefficient of headloss, the control strategy sets it to ξ_{\min} . The control force is regulated by varying the coefficient of headloss in accordance with the semi-active control strategy given as follows:

$$\begin{aligned} \xi(t) &= -2u(t)/(\rho A |\dot{X}_r| \dot{X}_r) \leq \xi_{\max} & \text{if } (u(t)\dot{X}_r(t)) < 0 \\ \xi(t) &= \xi_{\min} & \text{if } (u(t)\dot{X}_r(t)) \geq 0 \end{aligned} \quad (8)$$

In a fully active control system, one needs an actuator to supply the desired control force. In such a case, the control force is not constrained to be in the opposite direction to the velocity of the damper. Therefore, the linear control theory is readily applicable to active control systems. In case of semi-active systems, however, the proposed control law is a *clipped-optimal* control law since it emulates a fully active system only when the desired control force is dissipative [23,24]. Moreover, the actual supplied control force is dependent on the physical limitations of the valve used and the maximum coefficient of headloss it can supply, which means that there are bounds on the supplied control force, given as

$$\left(-\frac{\rho A \xi_{\min} |\dot{X}_r|}{2} \dot{X}_r \right) \leq u(t) \leq \left(-\frac{\rho A \xi_{\max} |\dot{X}_r|}{2} \dot{X}_r \right). \quad (9)$$

A slight variation of the above *continuously varying* orifice control is the often used *on–off* control. Most valve manufacturers supply valves that operate in the bi-state: fully open or fully closed. Such valves require a two-stage solenoid valve. On the other hand, the continuously varying control requires a variable damper which utilizes a servovalve. This servovalve is driven by a high response motor and contains a spool position feedback system, and therefore is more expensive and difficult to control than a solenoid valve. The on–off control is simply stated as

$$\begin{aligned} \xi(t) &= \xi_{\max} & \text{if } (u(t)\dot{X}_r(t)) < 0 \\ \xi(t) &= \xi_{\min} & \text{if } (u(t)\dot{X}_r(t)) \geq 0 \end{aligned} \quad (10)$$

ξ_{\min} can be taken as zero because this corresponds to the fully opened valve. It can be expected that a small value of ξ_{\max} will result in a lower level of response reduction.

Another common control strategy applicable to semi-active systems is fuzzy control. The basic idea behind fuzzy logic is that it allows a convenient way of representing input–output mapping in terms of human reasoning using verbose statements rather than mathematical equations. The whole process of fuzzy logic can be summarized as follows [25]: first the input and output variables are defined according to their respective *universe of discourse* (in a non-fuzzy crisp number system). The fuzzy sets are defined for each variable in terms of *membership functions*. These can be some mathematical functions (e.g., Gaussian, trapezoidal, etc.) and correspond to some state of the variable (e.g., small, large, etc.). The next step is to define a *fuzzy rule base* in terms of IF...THEN rules which relates the input and output in terms of verbal statements. Then the fuzzy logic goes through a series of processes starting with *fuzzification* where the crisp numbers are converted to fuzzy numbers, *fuzzy implication* where the inputs are mapped to output

membership functions, *fuzzy aggregation* where all output sets are combined into a single fuzzy output, and finally *defuzzification* where the fuzzy output is transformed back to a crisp number.

In order to formulate the system in state space, Eq. (2) can be written as

$$M\dot{x}(t) + Cx(t) + Kx(t) = E_1W(t) + B_1u(t), \quad (11)$$

which can be expressed in the state-space form as follows

$$\dot{X} = AX + Bu + EW, \quad (12)$$

where

$$X = \begin{bmatrix} x \\ \dot{x} \end{bmatrix},$$

$$A = \begin{bmatrix} 0 & I \\ -M^{-1}K & -M^{-1}C \end{bmatrix},$$

$$B = \begin{bmatrix} 0 \\ M^{-1}B_1 \end{bmatrix}$$

and

$$E = \begin{bmatrix} 0 \\ M^{-1}E_1 \end{bmatrix};$$

E_1 and B_1 are the control effect and loading effect matrices, respectively. The states of the system are the displacements and velocities of each lumped mass of the structure and the displacement and velocity of the liquid in the TLCD. The measurements of building response can be expressed as

$$Y = CX + Du + FW, \quad (13)$$

where $C=[I]$, $D=[0]$ and $F=[0]$ in the case of full state feedback. The desired optimal control force is generated by solving the standard LQR problem. The control force is obtained as follows

$$u = -K_g X, \quad (14)$$

where K_g is the control gain vector, given as

$$K_g = R^{-1}B^T P, \quad (15)$$

and P is the Riccati matrix obtained by solving the matrix Riccati equation

$$PA - PB(R^{-1}B^T P) + A^T P + Q = 0, \quad (16)$$

where Q and R are the control matrices for the LQR strategy. A schematic diagram of the control system is depicted in Fig. 2. The control performance of each strategy is evaluated under prescribed criteria. For this purpose, appropriate performance indices concerning the root-mean-square (RMS) displacements (y) and accelerations (\ddot{y}) of the structure and the effective control force (u) are defined below

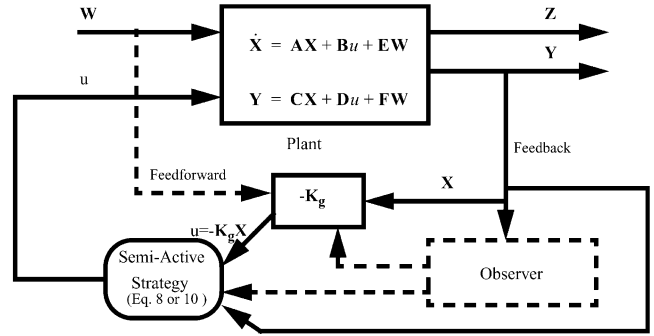


Fig. 2. Schematic of control system.

$$J_1 = \frac{(RMSy_{unco} - RMSy_{co})}{RMSy_{unco}}, \quad (17)$$

$$J_3 = \frac{(RMS\ddot{y}_{unco} - RMS\ddot{y}_{co})}{RMS\ddot{y}_{unco}}, \quad J_u = RMSu,$$

where subscripts *unco* and *co* are used to distinguish between uncontrolled and controlled cases.

In actual practice, it is more realistic to consider a few noisy measurements that are then used to estimate the system states. The standard stochastic LQG framework is used for estimation [26]. In a stochastic framework, the measurements are given as

$$Y = CX + Du + FW + v, \quad (18)$$

where v is the measurement noise which is invariably present in all measurements. From the measurements, the states of the system \hat{X} can be estimated using an observer

$$\dot{\hat{X}} = A\hat{X} + Bu + L(Y - C\hat{X} - Du), \quad (19)$$

where L is determined using standard Kalman filter estimator techniques. The optimal control is then written by

$$u = -K_g \hat{X}, \quad (20)$$

where K_g is the optimal control gain matrix obtained by solving the standard LQR problem as discussed previously. Substituting Eq. (20) into Eq. (19), the closed-loop form can be obtained as:

$$\dot{\hat{X}} = (A - BK_g - LC + LDK_g)\hat{X} + LY. \quad (21)$$

4. Example 1: MDOF system under harmonic loading

The first example, taken from Soong [27], is an MDOF-TLCD system as shown in Fig. 3. The lumped mass on each floor is 131,338.6 tons and the damping ratio is assumed to be 3% in each mode. The natural frequencies are computed to be 0.23, 0.35, 0.42, 0.49 and 0.56 Hz. A vector of harmonic excitation is defined:

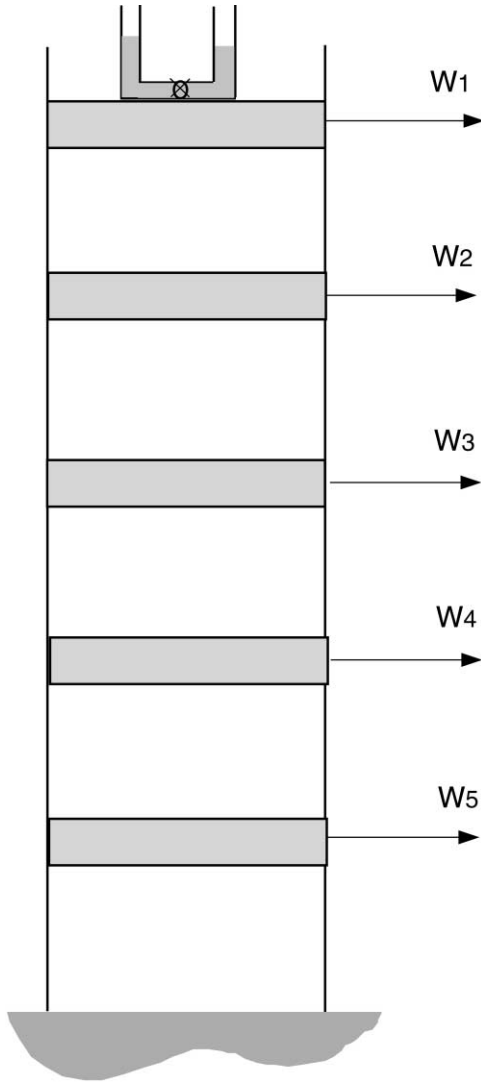


Fig. 3. Schematic of 5DOF building with semi-active TLCD on top story.

$$\mathbf{W}(t) = \mathbf{a} \cos(\omega t) + \mathbf{b} \cos(2\omega t) + \mathbf{c} \cos(3\omega t) + \mathbf{d} \sin(4\omega t), \quad (22)$$

where $\omega = 1.47$ rad/s (=first natural frequency of the structure), and the values of \mathbf{a} , \mathbf{b} , \mathbf{c} and \mathbf{d} and the stiffness matrix of the structure are given in Appendix B. The excitation acts at a frequency equal to the first natural frequency of the structure. The semi-active TLCD is placed on the top floor of the building. The TLCD is designed such that the ratio of the TLCD liquid mass to the first generalized mass of the building is 1%, the length ratio $\alpha = 0.9$ and $\xi_{\max} = 15$. Three cases of control strategies are considered: (1) full state feedback; (2) acceleration feedback; and (3) fuzzy controller using two measurements.

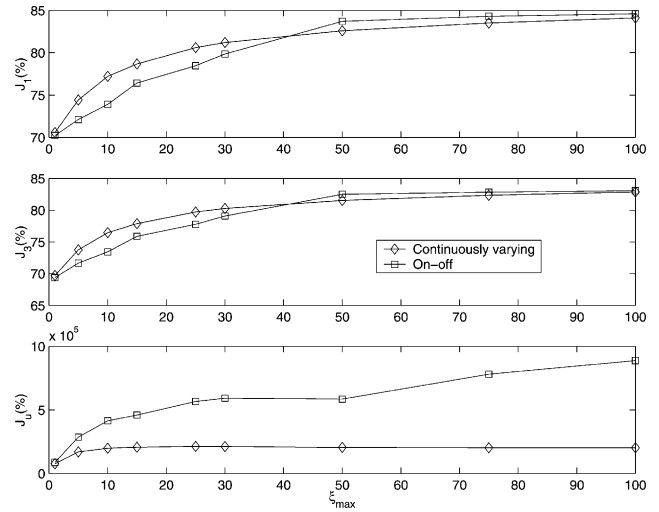


Fig. 4. Variation of performance indices with maximum headloss coefficient.

4.1. Full state feedback LQR strategy

The first strategy assumes that all states are available for feedback (total of 12 measurements). The control gains are calculated using Eq. (14). Fig. 4 shows the parametric variation of J_1 , J_2 and J_u as a function of ξ_{\max} . This can be understood from Eq. (9), which implies that the applied control force is constrained by ξ_{\max} . There are minor reductions in the response after a certain value of ξ_{\max} . This means that satisfactory control results can be achieved by choosing a valve that may have a limited range of headloss coefficients.

Fig. 5 shows the response of the top floor of the structure under various control strategies. One can note that the continuously varying and on-off strategies give similar reductions in response. This can be explained by

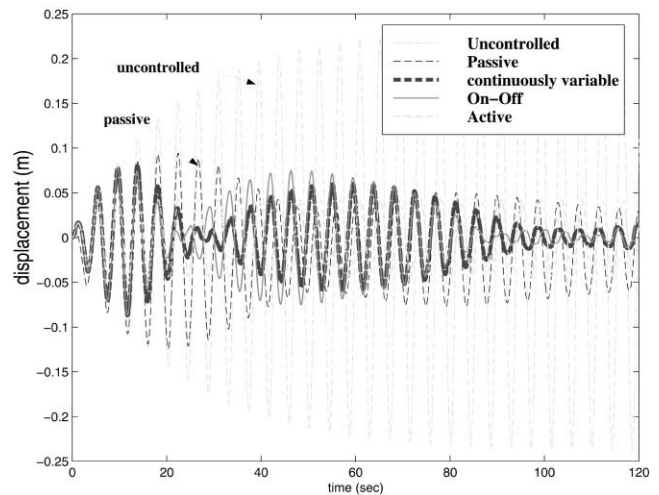


Fig. 5. Displacement of top floor under various control strategies.

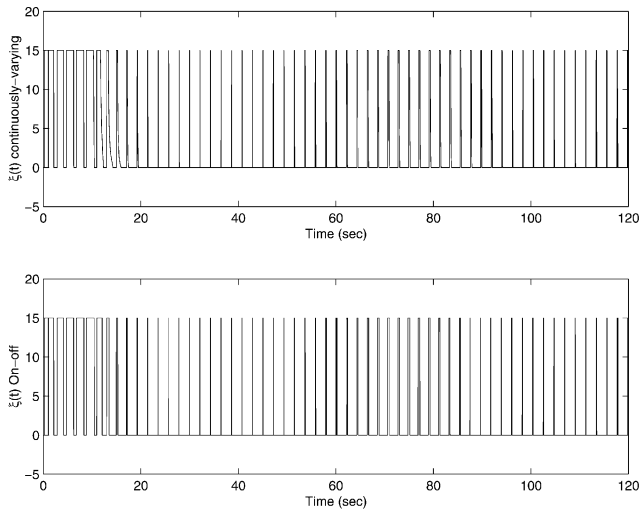


Fig. 6. Variation of headloss coefficient with time.

examining Fig. 6. The profiles of the variation in headloss coefficient as a function of time are similar for the two strategies. The continuously varying control gives flexibility in the headloss coefficient. However, the saturation bound introduces a clipping effect similar to on-off control and therefore, in this case, the advantage of the continuously varying control strategy is lost. Fig. 7 shows the RMS displacement of the floor displacements and accelerations, maximum story shear and maximum

inter-story displacements under various control strategies.

4.2. Observer-based LQG strategy

In the previous case, it was conveniently assumed that all the states are available for feedback. However, in practice only a limited number of measurements are feasible. In this case, we assume that the floor accelerations and the liquid level (displacement of the liquid) are measured. This implies that there is a total of six measurements (five accelerations and one liquid displacement). The measurement noises are modeled as Gaussian rectangular pulse processes with a pulse width of 0.002 s and a spectral density amplitude of $10^{-9} \text{ m}^2/\text{s}^3/\text{Hz}$. A comparison of the various strategies using observer-based LQG control is presented in Table 1. The response reduction is similar to the results obtained using the LQR control.

4.3. Fuzzy control strategy

In this section, a fuzzy controller is designed based on an on-off control strategy utilizing a limited set of measurements. The main focus is to demonstrate that a relatively simple intuitive control law can be generated using knowledge of the system dynamics. In this case, the relative importance of each state in the system is

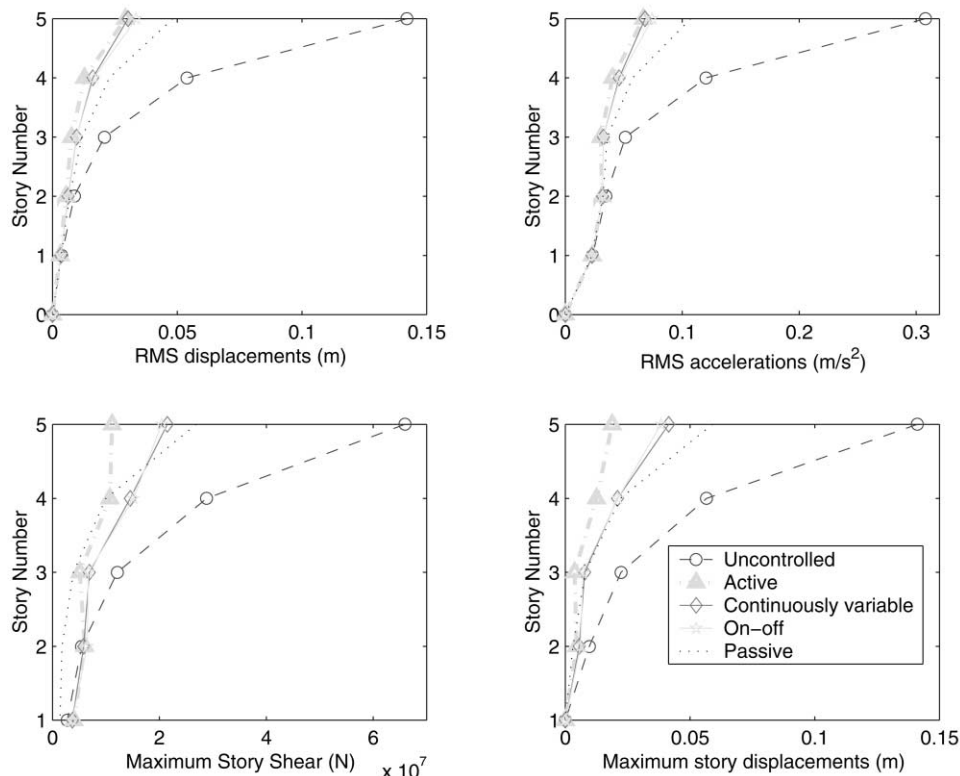


Fig. 7. Variation of RMS displacements, RMS accelerations, maximum story shear and maximum inter-story displacements.

Table 1
Comparison of various control strategies: Example 1

Control case	RMS displacement (cm) and (J_1 , %)	RMS acceleration (cm/s ²) and (J_3 , %)	RMS control force, J_u (kN)	Number of measurements
Uncontrolled	14.21	30.78	–	–
Passive TLCD	4.82 (66.08)	10.72 (65.17)	–	–
Active case	2.92 (79.45)	6.67 (78.33)	188 [Eq. (14)]	12
Continuously varying	3.03 (78.68)	6.81 (77.88)	171.6 [Eqs. (3) and (8)]	12
On–off control	3.35 (76.43)	7.43 (75.86)	203.1 [Eqs. (3) and (10)]	12
Continuously varying — observer based	3.21 (77.41)	7.58 (75.37)	70.4 [Eqs. (3) and (8)]	6
On–off control — observer based	3.13 (77.97)	8.43 (72.61)	170.7 [Eqs. (3) and (10)]	6
Fuzzy control	3.81 (73.18)	8.68 (71.8)	256.2 [Eqs. (3) and (25)]	2

weighted. The control force is then represented as a series of control terms which are subsequently discarded in actual implementation based on their relative weighting. One can rewrite the control force, in a state feedback scheme, in the following form:

$$u = - \sum_{i=1}^N k_i X_i, \tag{23}$$

where $\mathbf{K}_g = [k_1 k_2 \dots k_i \dots k_N]$ is the control gain vector obtained using Eq. (14). Depending on the weighting of the individual terms in the control force, one can write a sub-optimal control law of the form:

$$u \approx -k_l X_l, \tag{24}$$

where l is the subscript for the largest weighted state, i.e., the state which contributes the most to the control force in Eq. (23). Fig. 8(a) shows the plot of the relative weighting of the control gain vector of the different states. It is noted that the maximum contribution comes from the displacement of the top floor of the building, i.e., $X_7 = X_1$. The fuzzy controller implemented here is based on a modification of the on–off control law given in Eq. (10):

$$\begin{aligned} \xi(t) &= \xi_{\max} & \text{if } (X_f(t)\dot{X}_f(t)) < 0 \\ \xi(t) &= \xi_{\min} & \text{if } (X_f(t)\dot{X}_f(t)) \geq 0 \end{aligned} \tag{25}$$

From the control law given in Eq. (25), the inputs to the fuzzy controller are the displacement of the top story and the velocity of the damper. The output of the fuzzy controller is the coefficient of headloss. For each input and output, five trapezoidal membership functions corresponding to the NL (Negative Large), NS (Negative Small), ZO (Zero), PS (Positive Small) and PL (Positive Large) states are defined. The rule base of the controller was set up so that it emulated Eq. (25). The centroid method was chosen as the defuzzification method for obtaining the crisp output. The fuzzy controller was designed using MATLAB and its associated Fuzzy Logic Toolbox [28]. One can note that this strategy uses only two measurements as compared to the 12 measurements in the full state feedback case and six measure-

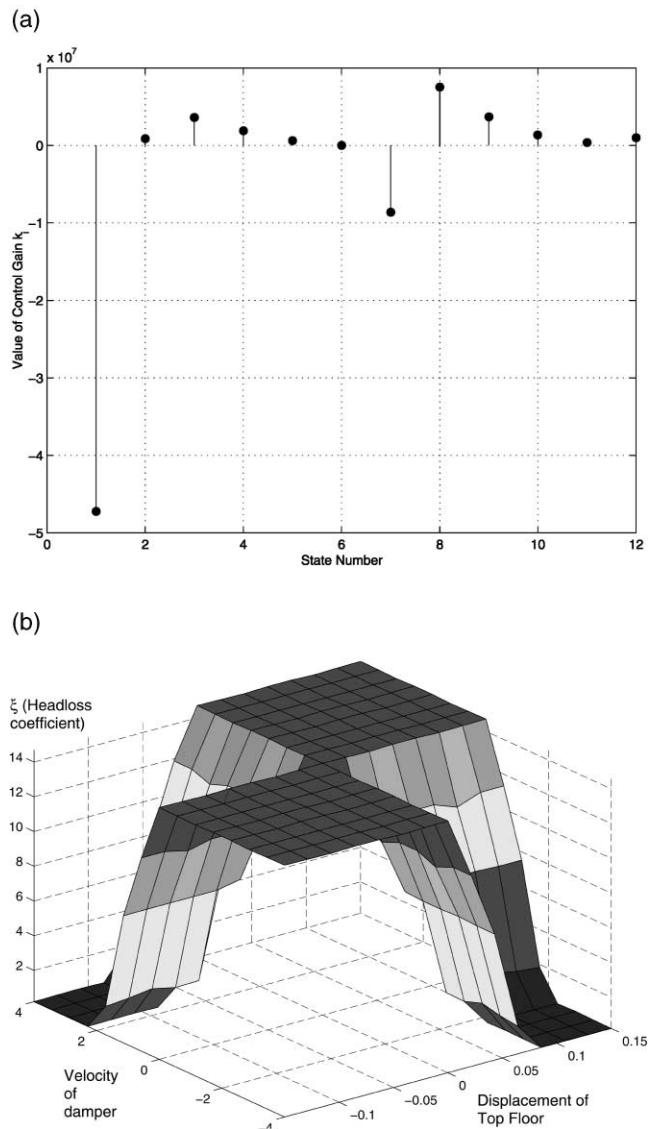


Fig. 8. (a) Comparison of control gains associated with each state; (b) control surface of fuzzy controller.

ments in the observer-based control case. Fig. 8(b) shows the fuzzy rule-base surface for the control law defined in Eq. (25), clearly showing the on–off nature of the algorithm.

5. Example 2: MDOF system under random wind loading

In this next example, we once again consider an MDOF-TLCD system which represents a high-rise building subjected to alongwind aerodynamic loading. The building dimensions are 31 m×31 m in plan and 183 m tall. The structural system is lumped at five levels and the eigenvalues of this building are found to be 0.2, 0.583, 0.921, 1.182 and 1.348 Hz. The modal damping ratios are 1%, 1.57%, 2.14%, 2.52% and 2.9%. The description of the wind loading and the structural system matrices for mass, stiffness and damping are given in Li and Kareem [29]. The semi-active TLCD is placed on the top floor of the building with similar parameters as in Example 1.

Using a multivariate simulation [30], wind loads were simulated at five levels, as shown in Fig. 9(a). Two types of semi-active strategy, namely the continuously varying and the on–off type controls, are examined. The LQR method, as described in the earlier section, is used to determine the control gains. It is assumed that all states are available for feedback.

The results are summarized in Fig. 9(b) and (c) and Table 2. As seen from Table 2, the semi-active strategies provide an additional 10–15% reduction over passive systems. Table 2 also shows how the two semi-active strategies deviate from the optimal control force. One can observe the sub-optimal performance of these schemes, in that they apply sub-optimal control force to the system, which leads to lesser response reduction than in the active case. In the case of the semi-active system, the applied control force is generated using a controllable valve which can be operated using a small energy source such as a battery.

6. Modeling valve dynamics

In the previous examples, the valve dynamics was excluded and an assumption of perfect tracking of the commanded voltage was invoked. However, in reality, the valve has its own dynamics which can affect the behavior of the damper if not properly modeled. The valve dynamics can be included in the overall system by measuring the valve–system response and fitting a model accordingly.

For example, experimental tests may yield a step response from which a second-order transfer function

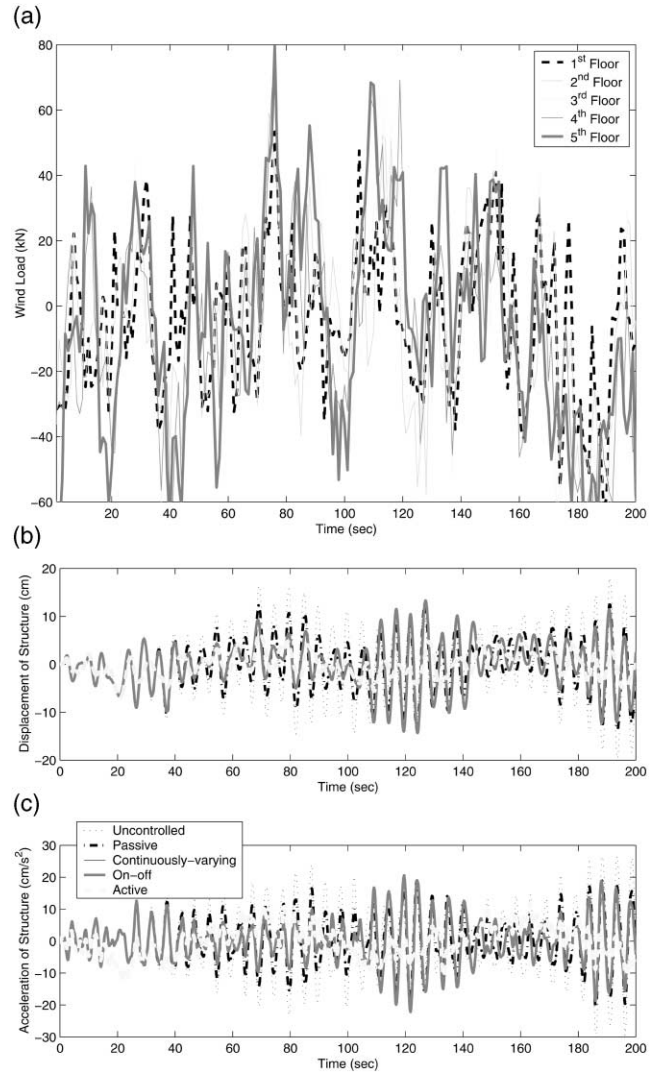


Fig. 9. (a) Wind loads acting on each lumped mass, (b) displacement and (c) acceleration of top level under various control strategies.

can be modeled that represents the valve dynamics. The transfer function can be written as (e.g., [31]):

$$H(s) = \omega_v^2 / (s^2 + 2\omega_v \zeta_v s + \omega_v^2). \quad (26)$$

Two cases are considered here. The first case involves a highly oscillatory response and a slow settling time for which the parameters of the model are taken as $\omega_v = 20$ rad/s and $\zeta_v = 0.3$, and the second case represents a damped response and a fast settling time with parameters $\omega_v = 200$ rad/s and $\zeta_v = 0.7$, respectively. The step response for each case and the resulting response of the top story are shown in Fig. 10(a) and (b). It is seen that the valve with fast dynamics has no effect on the response (error of 0.33% in RMS displacement response) while for the case in which the valve dynamics are slow and oscillatory, the effects are perceptible (error of 1.65% in RMS displacement response). Therefore, depending on the valve dynamics, one may or may not choose to include it in the overall system model.

Table 2
Comparison of various control strategies: Example 2

Control case	RMS displacement (cm) and (J_1 , %)	RMS acceleration (cm/s ²) and (J_3 , %)	RMS control force, J_u (kN)
Uncontrolled	7.05	10.61	–
Passive TLCD	5.24 (25.6)	7.63 (28.0)	–
Continuously varying	4.84 (31.2)	6.84 (35.3)	79.8 [Eqs. (3) and (8)]
On–off control	4.83 (31.2)	6.84 (35.3)	79.9 [Eqs. (3) and (10)]
Active control	2.51 (64.4)	4.87 (55.0)	133.8 [Eq. (14)]

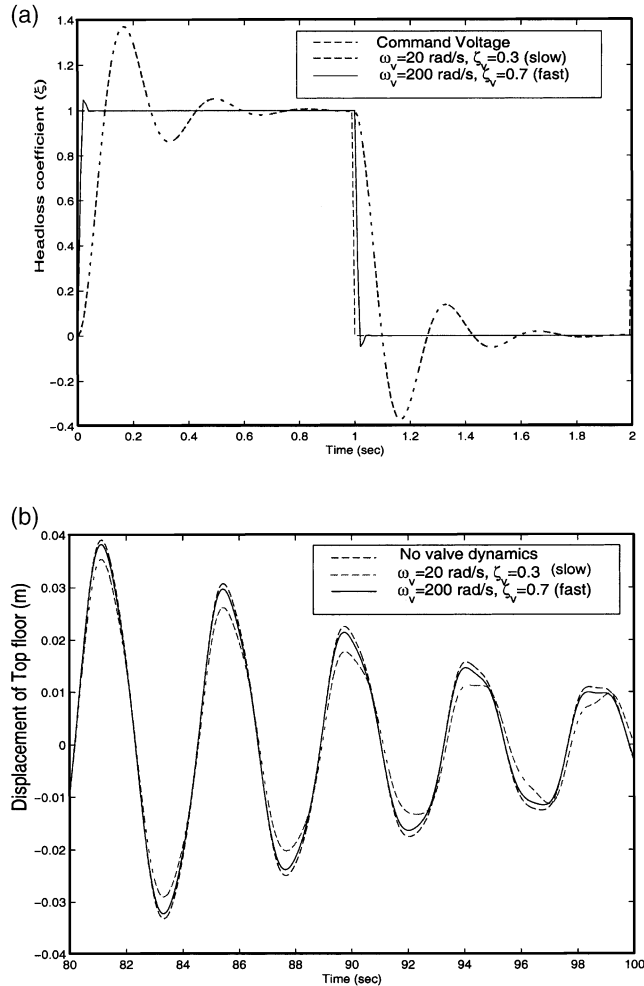


Fig. 10. (a) Step response for two different cases of valve dynamics; (b) effect on response of top story.

7. Concluding remarks

The following conclusions can be drawn from the study reported here.

1. The numerical simulations show that semi-active strategies provide a larger reduction in response than the passive systems. The power requirements for semi-active systems are negligible and the valve can be actuated by battery power. The efficiency of the

observer-based control strategy is shown where floor accelerations and liquid displacement are used as feedback variables. Numerical examples show that semi-active strategies provide better response reduction than passive systems for both random and harmonic excitations. In the case of harmonic loading the improvement is about 25–30%, while for random excitation the improvement is about 10–15%.

2. It is shown that the continuously varying semi-active control algorithm does not provide a substantial improvement in response reduction over the relatively simple on–off control algorithm.
3. Saturation is reached after a certain value of the maximum headloss coefficient. After this point, there is minor response reduction. This means that a valve which has a very high range of headloss coefficient may perform similar to a valve with a limited range of headloss coefficient.
4. Fuzzy control strategies can be implemented to obtain non-linear, intuitive, rule-based control objectives. In particular, the number of states to be measured can be reduced by understanding the dynamics of the system and taking note of the states which contribute significantly to the control force.

Acknowledgements

The authors gratefully acknowledge the support provided by NSF Grant CMS-95-03779.

Appendix A. Relation between C_v and ξ

Most valve suppliers provide a different measure of flow characteristic than the headloss coefficient (ξ) used in our paper. The commonly used measure is the valve conductance, which is defined as the mass flow of liquid through the valve, given by

$$Q = C_v \sqrt{\frac{\Delta p}{\eta}}, \quad (\text{A1})$$

where Q is the mass flow (kg/s); C_v is the valve conduc-

tance (m^2); η is the specific volume of the liquid (m^3/kg); and Δp is the pressure drop across the valve (Pa). The valve conductance is usually supplied in British rather than SI units. The parameter \tilde{C}_v in $gal/min/(psi)^{1/2}$ can be related to C_v by the equation:

$$C_v = 2.3837 \times 10^{-5} \tilde{C}_v. \quad (A2)$$

We can write the equation for the pressure loss as

$$\Delta p = \frac{gh_1}{\eta}. \quad (A3)$$

Substituting Eq. (4) for the headloss across the valve gives

$$\Delta p = \frac{\xi V^2}{2\eta}, \quad (A4)$$

so Eq. (A1) can be rewritten as follows:

$$\Delta p = \frac{\eta Q^2}{C_v^2}. \quad (A5)$$

The flow through the pipe of diameter D is given by:

$$Q = \frac{AV}{\eta} = \frac{\pi D^2}{4\eta} V. \quad (A6)$$

Comparing Eqs. (A4), (A5) and (A6), we obtain:

$$\xi = \frac{\pi^2 D^4}{8C_v^2}. \quad (A7)$$

Appendix B. Building parameters

The building stiffness matrix is given as:

$\mathbf{K} =$

$$0.0254 \begin{bmatrix} 2000 & -1000 & 0 & 0 & 0 \\ -1000 & 4800 & -1400 & 0 & 0 \\ 0 & -1400 & 6000 & -1600 & 0 \\ 0 & 0 & -1600 & 6600 & -1700 \\ 0 & 0 & 0 & -1700 & 7400 \end{bmatrix} \text{ kN/m}$$

and the excitation parameters in Eq. (22) are given as:

$$\mathbf{a} = 4.5 \begin{bmatrix} 675.45 \\ 700.45 \\ 615.15 \\ 555.25 \\ 475.05 \end{bmatrix} \text{ kN};$$

$$\mathbf{b} = 4.5 \begin{bmatrix} 0.3 \\ 375 \\ 284.5 \\ 175.3 \\ 15.1 \end{bmatrix} \text{ kN};$$

$$\mathbf{c} = 4.5 \begin{bmatrix} 735.5 \\ 655.15 \\ 564.45 \\ 690.15 \\ 18.6 \end{bmatrix} \text{ kN};$$

$$\mathbf{d} = 4.5 \begin{bmatrix} 180.5 \\ 35.5 \\ 425.0 \\ 280.0 \\ 650.05 \end{bmatrix} \text{ kN}.$$

References

- [1] Housner GW, Bergman LA, Caughey TK, Chassiakos AG, Claus RO, Masri SF et al. Structural control: past, present, and future. *J Eng Mech* 1997;123(9):897–971.
- [2] Hrovat D, Barak P, Rabins M. Semi-active versus passive or active tuned mass dampers for structural control. *J Eng Mech, ASCE* 1983;109(3):691–705.
- [3] Karnopp D. Design principles for vibration control systems using semi-active dampers. *J Dyn Syst Meas Control* 1990;112:448–55.
- [4] Ivers DE, Miller LR. Semi-active suspension technology: an evolutionary view. *Adv Automotive Technol, ASME* 1991;327:46.
- [5] Spencer BF Jr, Sain MK. Controlling buildings: a new frontier in feedback. *Emerging technologies [special issue]. IEEE Control Syst Mag* 1997;17(6):19–35.
- [6] Symans MD, Constantinou MC. Semi-active control systems for seismic protection of structures: a state-of-the-art review. *Eng Struct* 1999;21:469–87.
- [7] Kareem A, Kijewski T, Tamura Y. Mitigation of motions of tall buildings with specific examples of recent applications. *Wind Struct* 1999;2(3):132–84.
- [8] Sakai F, Takaeda S. Tuned liquid column damper — new type device for suppression of building vibrations. In: *Proceedings of International Conference on High Rise Buildings, Nanjing, China, 25–27 March 1989, 1989.*
- [9] Xu Y L, Samali B, Kwok KCS. Control of along-wind response of structures by mass and liquid dampers. *J Eng Mech* 1992;118(1):20–39.
- [10] Won AYJ, Pires JA, Haroun MA. Stochastic seismic performance evaluation of tuned liquid column dampers. *Earthquake Eng Struct Dyn* 1996;25:1259–74.
- [11] Kareem A. The next generation of tuned liquid dampers. In: *Proceedings of the First World Conference on Structural Control, vol I, Los Angeles, FB5. USA: IASC, 1994:19–28.*
- [12] Haroun MA, Pires JA. Active orifice control in hybrid liquid column dampers. In: *Proceedings of the First World Conference on Structural Control, vol. I, Los Angeles, FA1. USA: IASC, 1994:69–78.*
- [13] Yalla SK, Kareem A, Kantor JC. Semi-active control strategies for tuned liquid column dampers to reduce wind and seismic

- response of structures. In: *Proceedings of Second World Conference on Structural Control*, Kyoto, Japan. UK: John Wiley, 1998:559–68.
- [14] Yalla SK, Kareem A. Optimal absorber parameters for tuned liquid column dampers. *J Struct Eng*, ASCE 2000;126(8):906–15.
- [15] Lyons JL. *Lyons's valve designers handbook*. Van Nostrand Reinhold Co, 1982.
- [16] Symans MD, Constantinou MC. Experimental testing and analytical modeling of semi-active fluid dampers for seismic protection. *J Intell Mater Syst Struct* 1997;8(8):644–57.
- [17] Patten WN, Mo C, Kuehn J, Lee J. A primer on design of semi-active vibration absorbers (SAVA). *J Eng Mech*, ASCE 1998;124(1):61–8.
- [18] Kareem A, Gurley K. Damping in structures: its evaluation and treatment of uncertainty. *J Wind Eng Struct Aerodyn* 1996;59:131–57.
- [19] Yoshida K, Yoshida S, Takeda Y. Semi-active control of base isolation using feedforward information of disturbance. In: *Proceedings of Second World Conference on Structural Control*, Kyoto, Japan. UK: John Wiley, 1998:377–86.
- [20] Kurino H, Kobori T. Semi-active structural response control by optimizing the force–deformation loop of variable damper. In: *Proceedings of Second World Conference on Structural Control*, Kyoto, Japan. UK: John Wiley, 1998:407–17.
- [21] Sun L, Goto Y. Application of fuzzy theory to variable dampers for bridge vibration control. In: *Proceedings of the First World Conference on Structural Control*, Los Angeles, CA. USA: IASC, 1994:31–40.
- [22] Symans MD, Kelly SW. Fuzzy logic control of bridge structures using intelligent semi-active seismic isolation systems. *Earthquake Eng Struct Dyn* 1999;28:37–60.
- [23] Karnopp D, Crosby MJ, Harwood RA. Vibration control using semi-active force generators. *ASME J Eng Ind* 1974;96(2):619–26.
- [24] Dyke SJ, Spencer BF Jr., Sain MK, Carlson JD. Modeling and control of magnetorheological dampers for seismic response reduction. *Smart Mater Struct* 1996;5:565–75.
- [25] Passino KM, Yurkovich S. *Fuzzy control*. USA: Addison Wesley, Inc, 1997.
- [26] Maciejowski JM. *Multivariable feedback design*. UK: Addison-Wesley, Inc, 1989.
- [27] Soong TT. *Active structural control — theory and practice*. London and New York: Longman and Wiley, 1991.
- [28] Jang RJS, Gulley N. *Fuzzy control toolbox users guide*. Natick (MA): Mathworks, Inc, 1995.
- [29] Li Y, Kareem A. Recursive modeling of dynamic systems. *J Eng Mech*, ASCE 1990;116(3):660–79.
- [30] Li Y, Kareem A. Simulation of multi-variate random processes: hybrid DFT and digital filtering approach. *J Eng Mech*, ASCE 1993;119(5):1078–98.
- [31] Bateson RN. *Introduction to control system technology*. 6th ed. New Jersey: Prentice-Hall, 1999.
- [32] Abe M, Kimura S, Fujino Y. Control laws for semi-active tuned liquid column damper with variable orifice opening. Paper presented at 2nd International Workshop on Structural Control, Hong Kong, December 1996.